STAT1-cooperative DNA binding distinguishes type 1 from type 2 interferon signaling

Andreas Begitt[1,10], Mathias Droescher[1,9,10], Thomas Meyer[2,10], Christoph D Schmid[3,4], Michelle Baker[5], Filipa Antunes[1,9], Klaus-Peter Knobeloch[6], Markus R Owen[5], Ronald Naumann[7], Thomas Decker[8] & Uwe Vinkemeier[1]

STAT1 is an indispensable component of a heterotrimer (ISGF3) and a STAT1 homodimer (GAF) that function as transcription regulators in type 1 and type 2 interferon signaling, respectively. To investigate the importance of STAT1-cooperative DNA binding, we generated gene-targeted mice expressing cooperativity-deficient STAT1 with alanine substituted for Phe77. Neither ISGF3 nor GAF bound DNA cooperatively in the STAT1F77A mouse strain, but type 1 and type 2 interferon responses were affected differently. Type 2 interferon–mediated transcription and antibacterial immunity essentially disappeared owing to defective promoter recruitment of GAF. In contrast, STAT1 recruitment to ISGF3 binding sites and type 1 interferon–dependent responses, including antiviral protection, remained intact. We conclude that STAT1 cooperativity is essential for its biological activity and underlies the cellular responses to type 2, but not type 1 interferon.

Type 1 and type 2 interferons (IFNs) are key regulators of innate and adaptive immunity that exert their actions by modulating the expression of hundreds of genes[1]. Type 1 IFNs, which comprise IFN-β and several IFN-α isotypes, are secreted in response to viral infections by most cell types and induce a nonpermissive environment for virus replication. In contrast, the sole type 2 interferon, IFN-γ, is produced by macrophages and lymphocytes in the course of an overall immune response. It is best known as a potent activator of macrophages and their bactericidal activities. Interferon binding to membrane receptors activates Jak kinases, which trigger a cascade of tyrosine phosphorylation leading to the activation of STAT transcription factors. However, the different interferons activate different STAT signaling pathways[2]. Interferon-γ induces tyrosine phosphorylation of STAT1, generating SH2 domain–mediated homodimers (gamma-activated factor, or GAF) that bind to palindromic gamma-activated sequences (GAS). Type 1 IFNs, in contrast, induce structurally similar STAT1-STAT2 heterodimers, which require interferon-regulatory factor 9 (IRF9) for their function. The heterotrimeric complex, termed interferon-stimulated gene factor 3 (ISGF3) initiates transcription by binding to distinct IFN-stimulated response elements (ISREs). Type 1 IFNs also generate GAF to a minor extent, but assaying its relevance for signaling has been unfeasible to date. In addition to these canonical factors, both types of IFN can activate further STAT proteins and additional signaling pathways, but their contribution to IFN functions remains largely unknown[3].

GAF can recruit another GAF complex to adjacent GAS sites[4]. Similar polymerization, also referred to as cooperative DNA binding,

has been described for ISGF3 (ref. 5). GAF and ISGF3 polymerization each require STAT1 interactions, specifically with STAT1's amino-terminal (N) protein interaction domain, a structurally and functionally conserved entity unique to the STAT proteins[6]. The N domain is dispensable for SH2 domain–mediated dimerization of activated STATs and for binding of STATs to single DNA recognition sites[4,7,8]. Substitution of alanine for Phe77 in the N domain prevents cooperativity of GAF, but does not preclude gene transcription *per se*, as demonstrated by the continued ability to activate reporter genes driven by multiple high-affinity GAS sites[9]. Furthermore, the interface involving Phe77 mediates dimerization of unphosphorylated STAT1[10] in a conformation termed 'antiparallel'. Whereas unphosphorylated dimers adopt solely this conformation, tyrosine-phosphorylated dimers oscillate between the antiparallel conformation and the aforementioned structure stabilized by SH2-phosphotyrosine interactions, known as the parallel conformation. It is the parallel conformation that confers DNA binding activity[11].

Cooperative DNA binding is the basis for efficient switching between non-occupied and occupied promoter states. This principle is exemplified by phage λ repressor, whose cooperative binding to adjacent DNA sites translates a modest concentration decrease into an abrupt fall in promoter occupancy and transition to lytic growth[12]. To date, there have been few studies testing cooperativity mutants for the ability to fulfill their normal *in vivo* function. The available studies indicate that gene expression programs during animal development require switch-like responses as in λ phage, an example being Bicoid

cooperative DNA binding in *Drosophila melanogaster* embryonic patterning[13,14]. However, when graded responses to environmental stimuli are needed, such threshold effects on DNA binding may not be appropriate, as suggested by the small number of STAT5 cooperativity-dependent targets in interleukin 2 (IL-2) signaling and by the non-cooperative interactions that mediate transcription responses of inflammatory NF-κB[15,16]. The infrequency of IFN-regulated genes with clustered GAF or ISGF3 binding sites likewise implies a mere accessory role for STAT1 cooperativity in interferon signaling.

We generated gene-targeted mice with an F77A substitution in STAT1. Analysis of these mice revealed a pivotal role for cooperative DNA binding in interferon-controlled gene expression. However, type 1 and type 2 interferon immune responses were affected differently, in that antibacterial but not antiviral immunity was compromised. This outcome was explained by the need for STAT1 cooperativity for promoter recruitment of GAF but not ISGF3, and the GAF dependence on STAT1 cooperativity extended to target loci with only a single discernable STAT1 binding site. Our results furthermore indicated differences in the way the IFNs achieve gene repression. With the identification of single-site cooperativity, the characterization of mice expressing mutated STAT1 revealed a new facet in transcription factor–DNA interactions and an unexpected mechanistic diversity underlying type 1 and type 2 interferon–mediated immunity.

RESULTS

Generation of STAT1 cooperativity–deficient mice

To study the role of STAT1 cooperative DNA binding *in vivo*, we prepared a *Stat1* gene construct with the codon for Phe77 mutated to encode alanine, and targeted the *Stat1* locus of mouse embryonic stem (ES) cells for homologous recombination (**Supplementary Fig. 1a,b**) to generate homozygous *Stat1*[F77A/ F77A] animals (hereafter referred to as STAT1F77A mice). The generation of a gene-targeted mouse strain with an F77A substitution was verified by analysis of restriction fragment length polymorphism and by sequencing of genomic DNA (**Supplementary Fig. 1c,d**). STAT1F77A mutant mice, like STAT1-deficient mice[17], were viable in specific pathogen-free conditions.

Immunoblot analyses of spleen and embryonic fibroblasts (MEFs) from wild-type and STAT1F77A mice showed that STAT1 expression was similar in both mouse strains (**Fig. 1a**). The expression of STAT2 similarly was unaltered in STAT1F77A-derived MEFs, whereas IRF9 was elevated two- to threefold in these cells (**Fig. 1b,c**). Tyrosine phosphorylation of mutant STAT1F77A was slightly increased (1.5-fold) compared with wild-type STAT1 in response to both types of IFN (**Fig. 1b,c**), consistent with its diminished ability to adopt the antiparallel dimer conformation required for dephosphorylation[18]. The activation of STAT2 was normal (**Fig. 1c**).
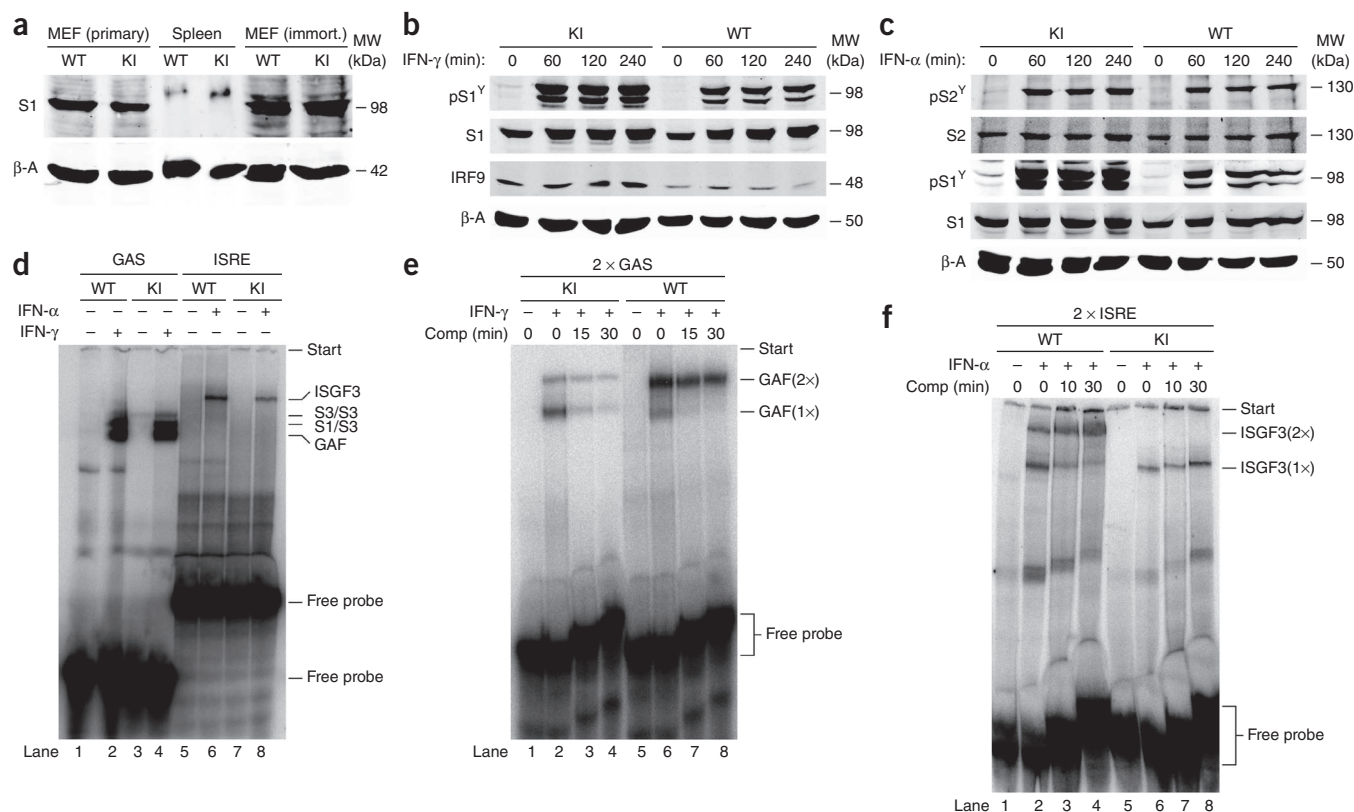
Figure 1 Both GAF and ISGF3 cannot bind DNA cooperatively in STAT1F77A mice. (**a**) Immunoblot analysis of total STAT1 (S1) in spleen (retarded mobility due to urea) and primary or SV40-immortalized (immort.) MEFs obtained from wild-type (WT, C57BL/6) and mutant (KI) mice. β-actin (β-A) was used as loading control. MW, molecular weight. (**b,c**) Immunoblot analysis of STAT1 phosphorylated at Tyr701 (pS1^Y), total STAT1 (S1), STAT2 phosphorylated at Tyr688 (pS2^Y), total STAT2 (S2), IRF9 and β-actin (β-A) in immortalized MEFs treated with IFN-γ (**b**) or IFN-α (**c**) for lengths of time indicated above blots (min). (**d**) EMSA using probes containing GAS or ISRE with extracts from immortalized MEFs treated with IFN-α or IFN-γ for 60 min (+) or left untreated (–). The positions of GAF, STAT1-STAT3 heterodimers (S1/S3), STAT3 homodimers (S3/S3), and ISGF3 are labeled. (**e,f**) Competition EMSA using probes containing tandem (2×) GAS (**e**) or ISRE (**f**) with extracts from immortalized MEFs stimulated with IFN-γ (**e**) or IFN-α (**f**) for 60 min. The samples in **e,f** were incubated with 500-fold molar excess of unlabeled probe for the indicated times (Comp (min)) before loading on the gel. Experiments were repeated at least three times (**a–f**).
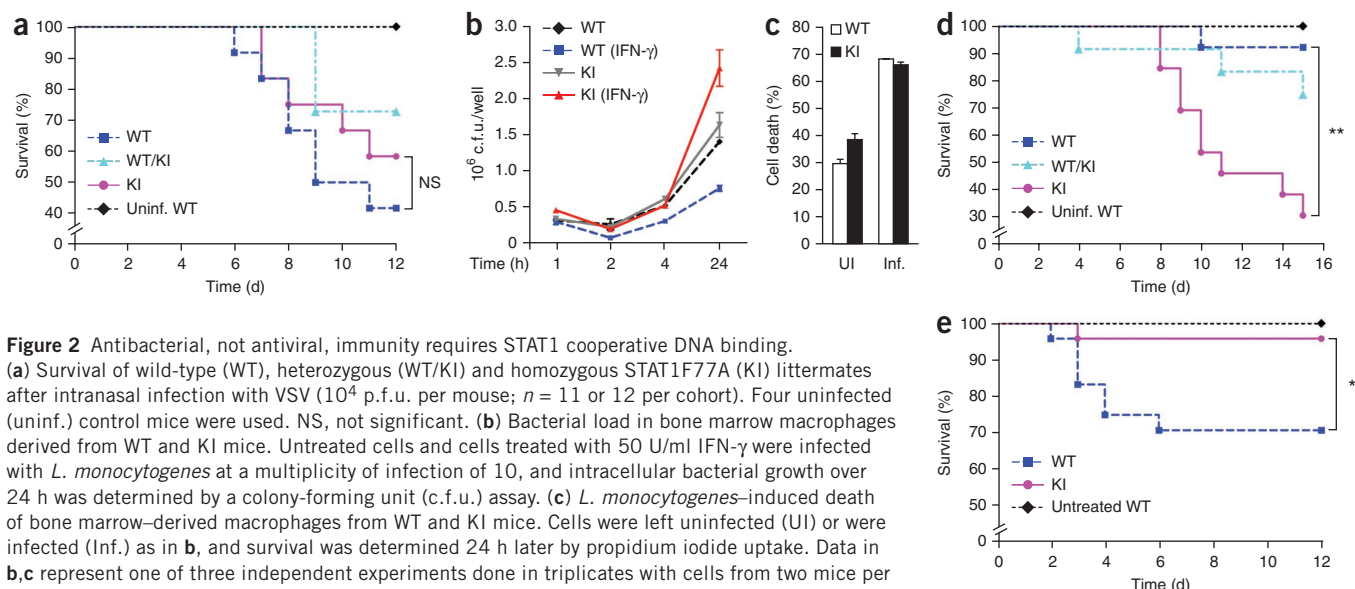
Figure 2 Antibacterial, not antiviral, immunity requires STAT1 cooperative DNA binding.
(**a**) Survival of wild-type (WT), heterozygous (WT/KI) and homozygous STAT1F77A (KI) littermates
after intranasal infection with VSV (10^4 p.f.u. per mouse; n = 11 or 12 per cohort). Four uninfected
(uninf.) control mice were used. NS, not significant. (**b**) Bacterial load in bone marrow macrophages
derived from WT and KI mice. Untreated cells and cells treated with 50 U/ml IFN-γ were infected
with *L. monocytogenes* at a multiplicity of infection of 10, and intracellular bacterial growth over
24 h was determined by a colony-forming unit (c.f.u.) assay. (**c**) *L. monocytogenes*–induced death
of bone marrow–derived macrophages from WT and KI mice. Cells were left uninfected (UI) or were
infected (Inf.) as in **b**, and survival was determined 24 h later by propidium iodide uptake. Data in
b,c represent one of three independent experiments done in triplicates with cells from two mice per
genotype. Line and bar graphs show means ± s.d. (**d**) Survival after intraperitoneal infection with
L. monocytogenes (1×10^6 c.f.u. per mouse; n = 12 to 14 per cohort including uninfected controls). (**e**) Survival after intraperitoneal injection with
Escherichia coli LPS (10 mg per kg body weight; n = 24 per cohort including untreated controls). *P = 0.022, **P = 0.001, log-rank (Mantel-Cox) test.
Experiments in **a,d** were done once; data in **e** are pooled from two independent experiments, each with 10–14 mice per genotype.

Next, we prepared whole-cell extracts for electrophoretic mobility
shift assays (EMSAs) with single GAS- or ISRE-containing probes
to assess the DNA binding activities of GAF and ISGF3. DNA
binding was unchanged for both the IFN-γ–induced GAF (**Fig. 1d**,
lanes 1–4) and IFN-α–induced ISGF3 (lanes 5–8). IFN-γ is also a
weak activator of STAT3 (ref. 19), as shown by additional slower-
migrating GAS-bound complexes constituting STAT3 homodimers
and STAT1-STAT3 heterodimers (**Fig. 1d**, lane 2). Comparison with
the banding pattern of STAT1F77A-derived extracts (lane 4) indi-
cated that STAT3 activation by IFN-γ and its heterodimerization with
STAT1 both were unaltered in the mutant MEFs.

Substantial differences between wild-type and STAT1F77A ani-
mals became evident when the binding to tandem GAS or ISRE was
probed. In wild type–derived extracts, both GAF (**Fig. 1e**, lanes 5–8)
and ISGF3 (**Fig. 1f**, lanes 1–4) formed, as expected, an additional
complex (2×) of reduced mobility. The 2× protein–DNA complexes
resisted competition with excess unlabeled binding sites better than
the respective single (1×) complexes, which is indicative of increased
DNA binding affinity. With STAT1F77A-derived cell extracts, how-
ever, the initial amounts of 2× GAF (**Fig. 1e**, lane 2) and 2× ISGF3
(**Fig. 1f**, lane 6) were much reduced compared with wild-type cell
extracts, and they did not show increased resistance to competition by
unlabeled probe (**Fig. 1e**, lanes 3 and 4, and **Fig. 1f**, lanes 7 and 8). We
concluded that the induction of GAF and ISGF3 and the binding to
their respective target sequences were unchanged in the STAT1F77A
mice, but the DNA-dependent cooperative multimerization of both
GAF and ISGF3 was abolished.
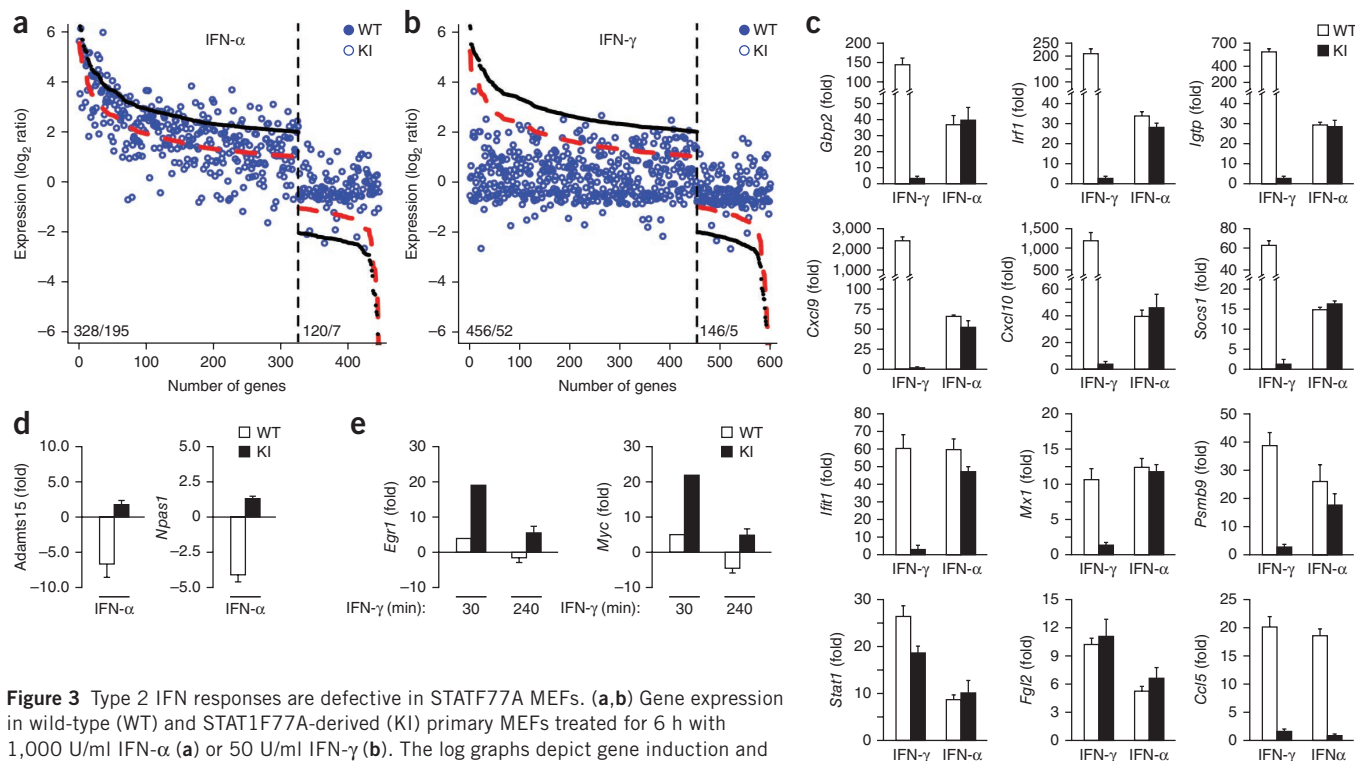
Type 1 and type 2 IFN responses in STAT1F77A mice
Interferons are critical for antiviral and antibacterial immunity,
which are compromised in patients and animals with STAT1 defi-
ciencies[17,20]. We infected wild-type and STAT1F77A mice with
vesicular stomatitis virus (VSV) as a model of IFN-α–mediated anti-
viral responses *in vivo*[21]. The mice succumbed to infection at similar
rates, 58% for wild-type mice and 42% for STAT1F77A mice (**Fig. 2a**).
This indicated that type 1 IFN–dominated responses do not require
STAT1 cooperativity.

Type 2 IFN, in contrast, activates macrophages to elicit anti-
bacterial protection, for instance against the intracellular pathogen
Listeria monocytogenes[22]. IFN-γ treatment of wild-type macrophages
reduced bacterial titers, whereas IFN-γ–treated macrophages from
STAT1F77A littermates did not curtail bacterial growth (**Fig. 2b**)
consistent with impaired production of cytotoxic nitric oxide in
STAT1F77A macrophages (**Supplementary Fig. 2**)[23]. Of note, type
1 IFNs have the opposite effect: they exacerbate listeriosis by induc-
ing apoptosis of macrophages. *Listeria*-induced apoptosis is therefore
reduced in STAT1-deficient macrophages compared with wild-type
macrophages[24]. STAT1F77A-derived macrophages, however, executed
this type 1 IFN–mediated process normally (**Fig. 2c**). *Listeria* infec-
tion of STAT1F77A mice confirmed that their antibacterial immunity
was significantly compromised. Of 13 infected STAT1F77A mice, only
4 survived, compared with 13 of 14 wild-type littermates (**Fig. 2d**).
Furthermore, STAT1F77A mice showed moderately increased resist-
ance to lipopolysaccharide (LPS)-induced septic shock (**Fig. 2e**), thus
phenocopying lack of STAT1 or IFN-γ rather than lack of type 1 IFN[25].
The *in vivo* results collectively indicated that defective STAT1 coop-
erativity affected type 1 and type 2 IFN responses differently, and
interfered with type 2 signaling specifically.

IFN-mediated gene transcription in STAT1F77A mice
We next assessed IFN-regulated gene expression associated with dis-
rupted STAT1 cooperativity. Selecting genes whose expression was
significantly altered (more than fourfold) after IFN treatment con-
firmed that the STAT1F77A mutation affected type 1 and type 2 IFN
signaling differently. In wild-type MEFs, IFN-α induced 328 genes
above the fourfold-change threshold. For 195 of these (59%), IFN-α–
induced expression in the STAT1F77A MEFs differed less than twofold
from wild-type and therefore was considered unchanged (**Fig. 3a**).
Those 195 genes included 67 of the 100 most strongly IFN-α–induced
genes in the wild-type MEFs; in contrast, none of the 100 most
strongly IFN-γ–induced genes retained undiminished expression in
STAT1F77A MEFs. Indeed, for 404 of the 456 IFN-γ–induced genes
(89%), expression was more than halved in the STAT1F77A cells
relative to wild-type (**Fig. 3b**). (The full gene lists for **Fig. 3a,b** are

Figure 3 Type 2 IFN responses are defective in STATF77A MEFs. (**a,b**) Gene expression in wild-type (WT) and STAT1F77A-derived (KI) primary MEFs treated for 6 h with 1,000 U/ml IFN-α (**a**) or 50 U/ml IFN-γ (**b**). The log graphs depict gene induction and repression as determined with dual-color microarrays. Vertical black dashed line separates induced genes (left) and repressed genes (right). Red dashed line marks twofold deviation from wild-type. Numbers within graphs indicate the number of IFN-regulated genes in wild-type cells, followed by a slash and then the number of these that are unaltered in STAT1F77A cells. (**c,d**) Gene induction (**c**) and repression (**d**) determined by quantitative RT-PCR in immortalized MEFs treated as in **a,b**. (**e**) Gene expression time course measured by quantitative RT-PCR in immortalized MEFs treated with IFN-γ for 30 min and 240 min. Microarray hybridizations (**a,b**) were done once; the data in **c**–**e** represent three independent experiments, except the 30-min time point in **e**, which was done once. Bars show mean and s.d.

provided in **Supplementary Tables 1** and **2**, respectively.) Quantitative RT-PCR validated the microarray results (**Fig. 3c** and **Supplementary Fig. 3a**), confirming that IFN-α–induced transcription was largely unperturbed in STAT1F77A MEFs, whereas IFN-γ responses were essentially lost. Notable exceptions included *Stat1* and *Fgl2*, which retained IFN-γ responsiveness, and *Ccl5* (also known as *Rantes*), which became unresponsive to either IFN (**Fig. 3c**).

IFN-α and IFN-γ repressed 120 and 146 genes, respectively, (**Fig. 3a,b,d,e** and **Supplementary Fig. 3b**). However, only 7 of the 120 genes repressed by IFN-α in wild-type remained IFN-α–repressible in the STAT1F77A cells. The situation was very similar for IFN-γ, with only 5 genes repressed in both wild-type and mutant cells (**Fig. 3a,b**). STAT1 cooperative DNA binding thus was indispensable for the gene-suppressive activities of both types of IFN; gene induction, in contrast, distinguished type 1 from type 2 IFN, as the former was largely unchanged by the loss of STAT1 cooperativity.

Recruitment of GAF and ISGF3 to IFN target genes

Transcription factor cooperativity facilitates switch-like gene regulation that interprets cellular signals in an all-or-none fashion, similarly to the STAT1 cooperativity that occurs in IFN-γ signaling. We examined promoter recruitment of GAF and ISGF3 using chromatin immunoprecipitation (ChIP). *Cxcl9* and *Tgtp1* are genes with tandem GAS sites in their promoters. IFN-γ induced recruitment of STAT1 in wild-type but not STAT1F77A-derived cells (**Fig. 4a** and **Supplementary Fig. 4a,b**). Indeed, defective STAT1 recruitment in STAT1F77A cells extended to genes with only single overt GAS sites, such as *Gbp2b* (*Gbp1*) (**Fig. 4b**), *Igtp*, *Socs1* and *Cxcl10* (**Supplementary Fig. 4c–e**).

In contrast, STAT1 associated normally with these promoters in response to IFN-α (**Fig. 4b** and **Supplementary Fig. 4c–e**). The corecruitment of STAT2 and IRF9 suggested mutant STAT1F77A was part of ISGF3 (**Fig. 4b** and **Supplementary Fig. 4c,e**). These results explained the different consequences of mutant STAT1F77A for IFN-γ– and IFN-α–induced gene expression shown in **Figure 3**.

To further dissect the requirements for GAF and ISGF3 promoter recruitment, we studied the *Irf1* promoter, where GAS and ISRE locate to separate promoter regions, unlike in the aforementioned genes. The *Irf1* proximal promoter harbors a single GAS site and recruited GAF but not ISGF3 (**Fig. 4c**). Conversely, the distal promoter contains a single ISRE and recruited ISGF3 but not GAF (**Fig. 4c**), affirming that GAF and ISGF3 recruitment requires their specific binding sites[26]. Moreover, on the *Irf1* proximal promoter (**Fig. 4c**) and the promoter of another gene, *Fgl2* (**Fig. 4d**), STAT1 was not detectable at GAS sites after IFN-α stimulation, consistent with a negligible role for GAF in type 1 IFN signaling. *Fgl2* was one of the few genes whose induction by IFN-γ remained unchanged in the STAT1F77A-derived cells (**Fig. 4c**). Here and in the promoter of *Irf9*—another gene with residual IFN-γ–induced transcription in STAT1F77A cells (**Supplementary Fig. 3a**)—ChIP experiments showed recruitment of the mutant GAF (**Fig. 4d** and **Supplementary Fig. 4f**). Thus, in certain gene contexts a single GAF sufficed for unknown reasons, but generally GAF required polymerization for gene induction, unlike ISGF3. ISGF3 could induce transcription without polymerizing, as shown by undiminished recruitment of ISGF3 to tandem ISREs in the *Ifit1* promoter (**Fig. 4e**).

The situation is less clear for IFN-mediated gene suppression. We tested genes that were repressed by IFN-α in wild-type but

Figure 4 Promoter recruitment of GAF, not ISGF3, requires STAT1 cooperativity. Gels show recruitment of complexes to promoters for *Cxcl9* (**a**), *Gbp2b* (**b**), *Irf1* (**c**), *Fgl2* (**d**), *Ifit1* (**e**), *Adamts15* (**f**), *Myc* (**g**) and *Egr1* (**h**), determined by ChIP analysis of nuclear preparations from immortalized wild-type (WT) and STAT1F77A MEFs (KI), before or after treatment with 1,000 U/ml IFN-α or 50 U/ml IFN-γ for 45 min. Anti-STAT1 (S1), anti-STAT2 (S2) or anti-IRF9 (IRF9) was used to immunoprecipitate (IP) the complexes, followed by PCR with primers designed to detect the promoters. The position and configuration of GAS and ISRE in each promoter sequence are indicated below the gels. bp, base pairs. Data are representative of two (**b**–**d**,**f**) or three independent experiments.

not STAT1F77A cells, namely *Adamts15* (**Fig. 4f**), *AldoB, Pvalb, Npas1* and *Pvrl4* (**Supplementary Figs. 4g** and **5a–c**). However, in both wild-type and STAT1F77A-derived cells, neither STAT1 nor STAT2 was recruited to these genes, irrespective of whether ISRE or GAS sequences were considered. This indicated that IFN-α–mediated gene repression did not involve ISGF3 or GAF. Nonetheless, STAT1 homotypic interactions were probably required, as mutant STAT1F77A cells did not show gene repression by IFN-α.

We also examined the recruitment of STAT1 to promoters of genes that become IFN-γ–inducible in both STAT1-deficient[27] and STAT1F77A cells; these genes include *Egr1, Myc* and *Jun* (**Fig. 3e** and **Supplementary Fig. 3b**). For *Myc* and *Jun*, IFN-γ–induced STAT1 recruitment was not established unambiguously (**Fig. 4g** and **Supplementary Fig. 5d**). The *Egr1* gene, however, showed cooperativity-dependent STAT1 recruitment, pointing to a direct role for multimerized GAF in gene suppression (**Fig. 4h**).

Multiple binding sites in target promoters are a hallmark of homotypic transcription factor cooperativity. STAT1 cooperativity, however, occurred at single GAS sites. Sequence analyses using position weight matrices[28] (PWM; **Supplementary Fig. 6**) as descriptors of binding preferences indicated at least one discernable GAS site in essentially all IFN-γ–upregulated genes (99%; **Supplementary Table 3**), but even under low-stringency conditions, tandem GAS sites were identified in only 70 IFN-γ–upregulated genes (15%) (**Supplementary Table 4**). We mathematically modeled DNA binding in a cooperative system with single or double GAS sites (**Supplementary Note**), in which the GAS sites are surrounded by non-GAS sites with a 50-fold difference in STAT-DNA binding affinity. Hence, the length of DNA was three sites in the single-GAS model and four sites in the double-GAS model. These models took into consideration that GAF is a symmetric molecule capable of open-ended polymerization[6]. Such modeling revealed that cooperativity reduced the transcription factor concentrations required to reach 99% GAS occupancy compared with non-cooperative binding, which would require 13-fold higher concentrations to achieve the same factor occupancy (**Fig. 5a**). Even if the affinities of STAT1 for GAS and non-GAS sites differed
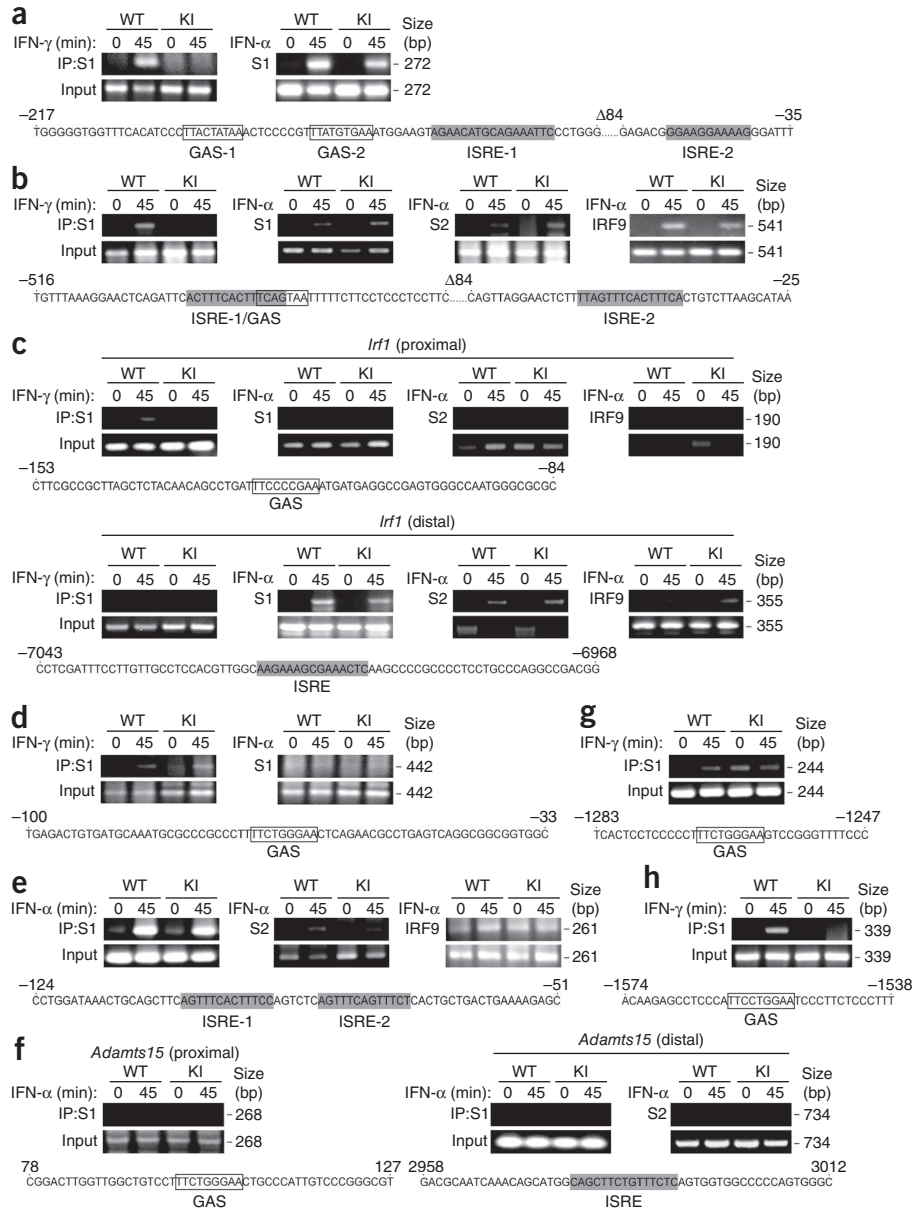
200-fold, cooperativity still markedly increased promoter occupancy (**Supplementary Fig. 7a**). The predicted outcome was very similar when a conventional tetramer model with just two binding sites was used (**Supplementary Fig. 7b**).

We therefore asked whether we could rescue IFN-γ–induced promoter recruitment and gene transcription in the cells of STAT1F77A mice by increasing the STAT1 concentration. This experiment mimicked an immune response in which cells are exposed for prolonged periods of time to low doses of IFN-γ, a process called IFN-γ priming that can be induced under cell-culture conditions[29]. IFN-γ priming for 24 h increased STAT1 concentrations in both wild-type and STAT1F77A-derived MEFs about fivefold (**Fig. 5b**, middle), which in turn raised subsequent STAT1 activation by IFN-γ about threefold (data not shown). In wild-type cells, IFN-γ priming accordingly led to variably heightened gene expression. Yet priming did not rescue defective gene expression in STAT1F77A-derived MEFs, the *Stat1* gene being a notable exception (**Fig. 5c**). In the mutant cells, priming likewise did not correct the loss of STAT1 promoter recruitment (**Fig. 5d**–**f**). These results demonstrated that STAT1 cooperative DNA binding was
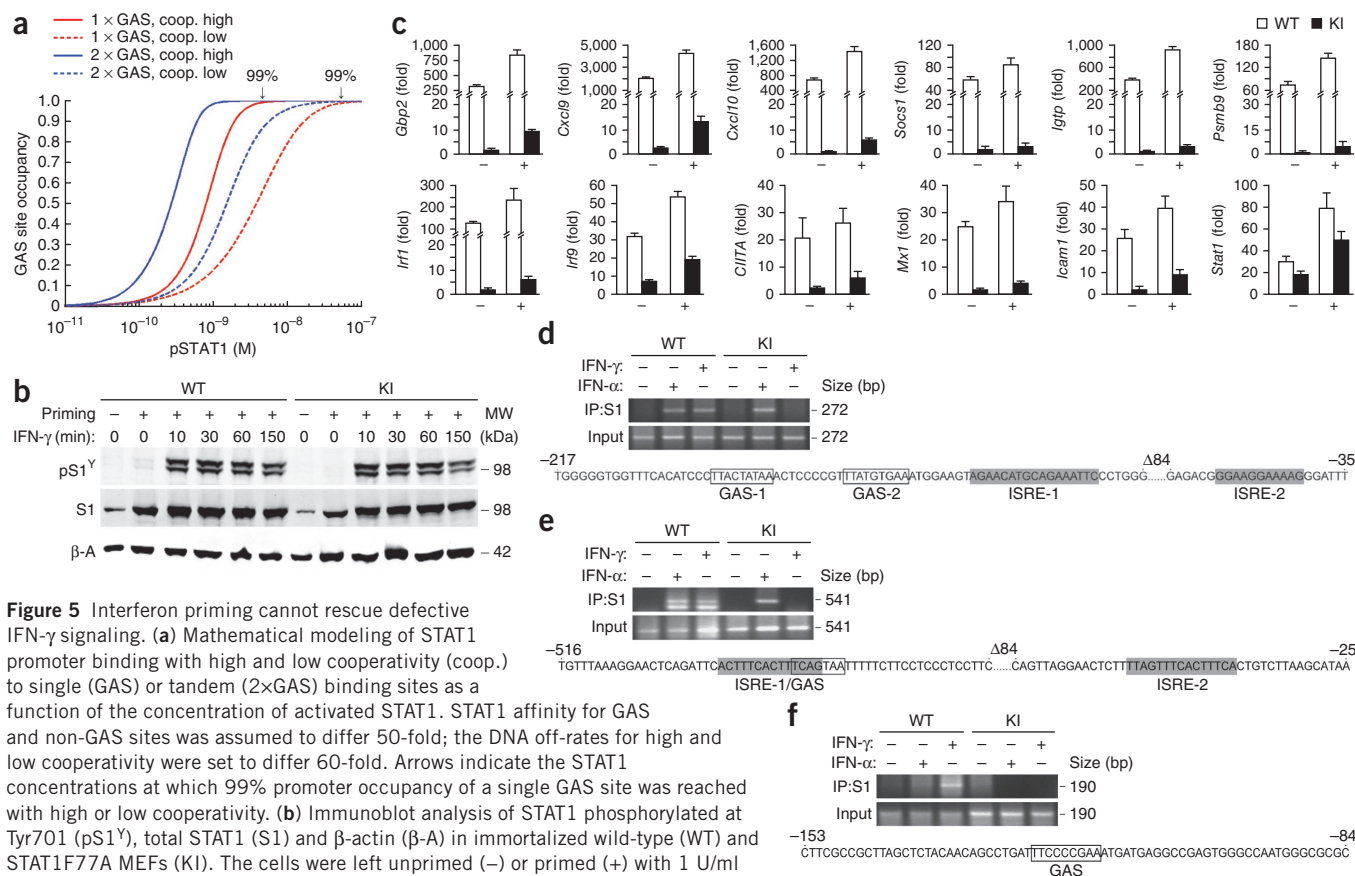
Figure 5 Interferon priming cannot rescue defective IFN-γ signaling. (**a**) Mathematical modeling of STAT1 promoter binding with high and low cooperativity (coop.) to single (GAS) or tandem (2×GAS) binding sites as a function of the concentration of activated STAT1. STAT1 affinity for GAS and non-GAS sites was assumed to differ 50-fold; the DNA off-rates for high and low cooperativity were set to differ 60-fold. Arrows indicate the STAT1 concentrations at which 99% promoter occupancy of a single GAS site was reached with high or low cooperativity. (**b**) Immunoblot analysis of STAT1 phosphorylated at Tyr701 (pS1^Y), total STAT1 (S1) and β-actin (β-A) in immortalized wild-type (WT) and STAT1F77A MEFs (KI). The cells were left unprimed (−) or primed (+) with 1 U/ml IFN-γ for 24 h before addition of 50 U/ml IFN-γ for lengths of time indicated above blots (min). MW, molecular weight. (**c**) Gene expression as determined by quantitative RT-PCR using immortalized MEFs left unprimed (−) or primed (+) as in **b**, followed by the addition of 50 U/ml IFN-γ for 6 h. Bars show mean and s.d. (**d–f**) ChIP with anti-STAT1 (S1) of nuclear preparations from immortalized MEFs primed with IFN-γ as in **b**, followed by treatment without (−) or with (+) 1,000 U/ml IFN-α or 50 U/ml IFN-γ for 45 min. After ChIP, PCR was done with primers designed to detect promoters of Cxcl9 (**d**), Gbp2b (**e**) and Irf1 (**f**). The position and configuration of GAS and ISRE in the respective promoter regions are indicated. IP, immunoprecipitate; bp, base pairs. Data are representative of two (**b**,**d–f**) or three (**c**) independent experiments.

dispensable for the promoter recruitment of ISGF3. GAF, in contrast, was dependent on it, irrespective of the presence of multiple STAT1 binding sites. Our conclusion that single-site cooperativity substantially enhanced STAT1 promoter recruitment was supported by both theoretical and experimental considerations, namely mathematical modeling and IFN-γ priming experiments.

Chromatin recruitment of cooperativity-deficient STAT1

The above experiments demonstrated that introduction of alanine at position 77 prevented STAT1 recruitment specifically to IFN-γ–regulated promoters, but they could not clarify whether the defect generally precluded STAT1-chromatin interactions. To answer this question, we took advantage of a well-characterized phenomenon reliant on STAT1-chromatin interactions, namely the retention of activated STAT1 in the nucleus of cytokine-stimulated cells[30]. To make nuclear retention a direct readout of STAT1-chromatin interactions, we needed to bypass the second known contributor to nuclear retention—the inability of activated STAT1 to return to the cytoplasm[30]. We achieved this by fusing a nuclear export signal (NES) to the STAT1 C-terminus, in a construct termed STAT1-NES[31] (**Supplementary Fig. 8a**), which results in enhanced STAT1 activation after IFN stimulation (**Supplementary Fig. 8b**). In addition to wild-type and STAT1F77A, we tested two previously characterized mutants with altered DNA binding, namely mutant DNA[minus], which has entirely lost DNA binding, and mutant DNA[plus] with

sequence-nonspecific DNA binding[32]. The variants were tagged with green fluorescent protein (GFP), and the extent of STAT1 nuclear retention was determined in HeLa cells by quantitative confocal microscopy. In unstimulated cells, all the STAT1-variant NES-fusion proteins were predominantly cytoplasmic, as expected (**Supplementary Fig. 8c**). The nuclear GFP signal accordingly was very low (**Fig. 6a**, lanes 2–6). Treatment with IFN-γ or IFN-α significantly increased the nuclear signal for wild-type STAT1 (**Fig. 6a**, lanes 7 and 12). This increase was entirely dependent on STAT1-DNA interactions, as it was lost with mutant DNA[minus] (**Fig. 6a**, lanes 8 and 13). This outcome was consistent with the requirement of both GAF and ISGF3 for STAT1-DNA contacts to bind DNA[33], and it showed that IFN-inducible nuclear GFP fluorescence of STAT1-NES was a direct readout for STAT1 chromatin binding. Mutation F77A was tested next. It, too, prevented STAT1 nuclear retention, but only in response to IFN-γ, not IFN-α, which mirrored the ChIP results (**Fig. 6a**, lanes 9 and 14). DNA interactions thus were necessary and sufficient for nuclear retention of IFN type 1–activated STAT1, presumably ISGF3, while retention of type 2–induced STAT1, presumably GAF, required cooperativity in addition. In an extension of our gene-selective ChIP results, the imaging experiments thus showed globally disrupted STAT1 recruitment to IFN-γ target genes. Given this exhaustive chromatin-binding deficiency, we tested whether impaired Ser727 phosphorylation of STAT1 contributed to IFN-γ malfunctioning in STAT1F77A mice, as this transcription-augmenting modification has been proposed to require
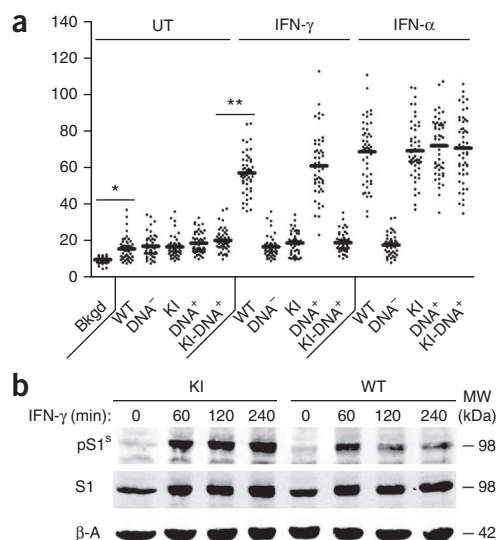
Figure 6 Effects of mutation F77A on STAT1 chromatin association and serine phosphorylation. (**a**) Quantitative confocal microscopy recordings of GFP signal intensities in the nucleus of HeLa cells transfected with GFP-tagged STAT1-NES (WT) and various mutants (KI, F77A; DNA+, DNA^{plus}; DNA−, DNA^{minus}). The scatterplots each depict unprocessed nuclear GFP signals of 50 randomly selected eligible cells left untreated (UT) or treated with 50 U/ml IFN-γ or 1,000 U/ml IFN-α for 60 min. Bkgd, background fluorescence in untransfected cells. Horizontal bars indicate average fluorescence intensity. *$P < 0.01$, **$P < 0.001$, Student's t-test. (**b**) Immunoblot analysis of STAT1 phosphorylated at Ser727 (pS1^S), total STAT1 (S1) and β-actin (β-A) in immortalized MEFs from wild-type and STAT1F77A (KI) mice treated with IFN-γ for lengths of time indicated above blots (min). Data are representative of two (**a**) or three (**b**) independent experiments.

STAT1 chromatin tethering[34]. However, IFN-γ–induced Ser727 phosphorylation of mutant STAT1 was undiminished compared with wild-type, ruling out this possibility (**Fig. 6b**).

We then tested mutant DNA^{plus}, which has sequence-nonspecific DNA binding, to investigate whether STAT1 chromatin association mandated the recruitment to GAS or ISRE. However, both GAF and ISGF3 complexes containing this STAT1 variant were still retained in the nucleus (**Fig. 6a**, lanes 10 and 15). Finally, the substitution F77A was introduced in mutant DNA^{plus}, which resulted in the loss of STAT1 nuclear retention in response to IFN-γ (**Fig. 6a**, lane 11) but not IFN-α (**Fig. 6a**, lane 16). We concluded that the F77A substitution generally disrupted the chromatin recruitment of GAF—that is, irrespective of the presence of GAS sites. Chromatin recruitment of ISGF3, in contrast, generally occurred independently of STAT1 cooperativity, and hence irrespective of recruitment to ISRE sites. These findings further support the idea that loss specifically of STAT1 homotypic interactions, rather than disruption of other STAT1-promoter interactions, was responsible for defective IFN-γ signaling in the STAT1F77A mice. **Supplementary Figure 9** summarizes these results.

DISCUSSION

Cooperative DNA binding is a fundamental mechanism in gene regulation, yet the consequences of defective cooperativity for normal *in vivo* functions have been tested for very few transcription factors. The available results have raised the possibility that cellular responses to environmental challenges might, instead, rely on analog, non-cooperative transcriptional control to accurately reflect stimulus

strength[16]. Here we showed that STAT1 cooperative DNA binding was indispensable for IFN-γ signaling and antibacterial immunity owing to a pervasive promoter recruitment defect. STAT1 dimers are not the transcriptionally active unit for the vast majority of IFN-γ–regulated genes, in stark contrast to STAT5 dimers in IL-2 signaling[15]. STAT1 functioning thus demonstrated that the principles of cooperativity, originally identified in the repressor protein of phage λ, are embodied largely unaltered in an extracellular signal-regulated mammalian transcription factor. Yet, in contrast to λ repressor and other examples of cooperativity, STAT1 cooperative DNA binding did not require clustered binding sites. As our data did not allow *de novo* binding site discovery, we searched the promoter regions of the mouse genome for the presence of multiple canonical GAS motifs using bioinformatics tools to assess the sequence requirements of GAF polymerization. This analysis indicated that although GAS sites are a frequent occurrence, multiple GAS sites are rare even when very relaxed sequence constraints are applied; and multiple GAS sites were also not found to be enriched in IFN-γ target genes that require GAF polymerization. Combining these findings with genome-wide studies, which underscored the importance of GAS for IFN-γ–induced STAT1 promoter recruitment[35], we conclude that STAT1 polymerization originates from GAS and then proceeds with very loose, if any, additional sequence constraints. This is consistent with studies of *in vitro* DNA binding, in which recruitment of multiple dimers to a single GAS site is observed[9], and with the relatively high affinity of STAT1 N-domain interactions (K_d ~20 μM)[11]. These results indicate that researchers still have limited ability to infer the structure or composition of DNA sequence–specific transcription complexes from the configuration of binding sites[36]. As protein-protein interactions between DNA-bound proteins are integral to transcription initiation, the uncoupling of transcription factor binding and DNA sequence specificity observed here for STAT1 may be of wider significance in transcription regulation than is currently appreciated.

Mathematical modeling indicated that cooperativity allows wild-type STAT1 to function at more than tenfold reduced concentration compared with the cooperativity-deficient mutant, in line with the IFN-γ priming experiments, in which about a threefold increase in STAT1 concentration was insufficient for rescuing defective promoter recruitment. The concentration of activated STAT1 is a function of IFN-γ signal strength, so that cooperative DNA binding defines a minimal signal threshold necessary to tip the balance from unoccupied to occupied promoter states. As GAF polymerization is driven more by protein-protein interactions than by sequence-specific DNA binding, a single GAS site is all that is required for different genes to reach the tipping point at the same signal strength, thus effectively synchronizing cellular IFN-γ–regulated gene expression.

Type 1 IFN–activated STAT1F77A, in contrast, was readily recruited to chromatin—including to neighboring sites not bound in response to IFN-γ—albeit as part of ISGF3. As STAT1 activation was similar with either IFN, its recruitment via ISGF3 was more efficient compared with GAF. It is unlikely that this difference is explained by the ability of ISGF3 to utilize interactions with other IFN promoter–specific proteins, as polymerization-independent chromatin recruitment was not limited to IFN-regulated promoters. Instead, the inherent DNA binding characteristics may explain the greater binding efficiency of ISGF3. The data on ISGF3 DNA binding are compatible with a model in which ISGF3 itself is the product of cooperative DNA binding, namely between STAT1-STAT2 heterodimers and IRF9, which each bind to distinct nucleotides within the ISRE[33,37,38]. The fundamental difference between GAF and ISGF3, therefore, is probably not the need for cooperative DNA binding, but rather the need

for polymerization. The requirement of GAF polymerization for productive promoter binding suggests lower affinity or shorter-lived chromatin interactions compared with ISGF3. The chromatin residence time of STAT1 increases ~100-fold upon IFN-γ stimulation, lasting up to several seconds[39]. Although these numbers likely represent GAF polymers, the relationship between signal strength and polymer length on one hand, and transcription output on the other, remains unknown. It is tempting, though, to speculate that the three processes are directly proportional, so that IFN-γ signaling, once the minimal signal threshold is reached, adopts analog characteristics whereby polymer length gauges signal strength. In contrast, ISGF3 polymerization was not required for the induction of most type 1 IFN–regulated genes. Nonetheless, ISGF3 was polymerization competent, and this activity may be required in certain instances—for example, for induction of genes such as *Ccl5* that were induced by type 1 IFNs in wild-type but not STAT1F77A cells. Another situation where polymerization could be required is transcription regulation by unphosphorylated ISGF3 (ref. 40). This recently characterized transcription regulator with presumably weakened DNA binding compared with 'classical' ISGF3 may necessitate stabilization through polymerization for productive chromatin interactions. It is worth noting that while STAT1 mutation F77A had little consequence for IFN-α–mediated gene induction, the effects on gene repression were extensive. However, gene repression did not seem to entail DNA binding of ISGF3 components, which is in accord with a published report that ascribes IFN-α–mediated downregulation to secondary effects[41]. In contrast, IFN-γ–mediated gene repression and gene induction seemed to share the requirement for STAT1 cooperativity, and hence GAF polymerization. A scenario where the single transcription factor functions as an inducer and the polymer as repressor, as proposed for STAT5 (ref. 42), therefore is implausible for STAT1.

The opposing polymerization requirements of GAF and ISGF3 enabled us to dissect their biological functions. Genes such as *Gbp2*, *Cxcl10* or *Ifit1*, which became IFN-γ unresponsive in STAT1F77A cells, retained undiminished responsiveness to IFN-α. Under our experimental conditions we thus found no evidence for a contribution of GAF to type 1 IFN signaling. Rather, the functional analyses of STAT1F77A mice highlighted the distinct functions of GAF and ISGF3 in antibacterial and antiviral immunity, respectively. Moreover, the polymerization dependence of GAF but not ISGF3 identifies the STAT1 N domain as a potential candidate target for suppressing STAT1-mediated IFN-γ activities without compromising antiviral immunity. In conclusion, we showed that STAT1 cooperative DNA binding has a minor role in type 1 IFN responses and antiviral immunity, but is indispensable for type 2 IFN responses and antibacterial immunity.

METHODS

Methods and any associated references are available in the online version of the paper.

Accession codes. GEO: microarray data, GSE49441; BioModels: mathematical models, MODEL1311130000 and MODEL1311130001.

Note: Any Supplementary Information and Source Data files are available in the online version of the paper.

AUTHOR CONTRIBUTIONS

A.B. designed and executed gene expression and promoter binding studies; M.D. and T.M. generated the STAT1F77A mouse strain, and designed and performed biochemical experiments and animal studies; C.D.S. did bioinformatics promoter analyses; M.B. and M.R.O. generated mathematical models; F.A. designed and performed cell-based assays and generated microarray data; K.-P.K. and R.N. contributed reagents and expertise for mouse genetics experiments; T.D. provided reagents and expertise for bacterial infection experiments; U.V. conceived the research, directed the study and wrote the manuscript. All authors contributed to data analyses and manuscript editing.

1. Stark, G.R., Kerr, I.M., Williams, B.R., Silverman, R.H. & Schreiber, R.D. How cells respond to interferons. *Annu. Rev. Biochem.* **67**, 227–264 (1998).
2. Stark, G.R. & Darnell, J.E. Jr. The JAK-STAT pathway at twenty. *Immunity* **36**, 503–514 (2012).
3. Platanias, L.C. Mechanisms of type-I- and type-II-interferon-mediated signalling. *Nat. Rev. Immunol.* **5**, 375–386 (2005).
4. Vinkemeier, U. *et al.* DNA binding of in vitro activated Stat1 alpha, Stat1 beta and truncated Stat1: interaction between NH2-terminal domains stabilizes binding of two dimers to tandem DNA sites. *EMBO J.* **15**, 5616–5626 (1996).
5. Li, X., Leung, S., Burns, C. & Stark, G.R. Cooperative binding of Stat1-2 heterodimers and ISGF3 to tandem DNA elements. *Biochimie* **80**, 703–710 (1998).
6. Vinkemeier, U., Moarefi, I., Darnell, J.E. Jr. & Kuriyan, J. Structure of the amino-terminal protein interaction domain of STAT-4. *Science* **279**, 1048–1052 (1998).
7. Xu, X., Sun, Y.L. & Hoey, T. Cooperative DNA binding and sequence-selective recognition conferred by the STAT amino-terminal domain. *Science* **273**, 794–797 (1996).
8. Bonham, A.J. *et al.* STAT1:DNA sequence-dependent binding modulation by phosphorylation, protein:protein interactions and small-molecule inhibition. *Nucleic Acids Res.* **41**, 754–763 (2013).
9. Meyer, T., Hendry, L., Begitt, A., John, S. & Vinkemeier, U. A single residue modulates tyrosine dephosphorylation, oligomerization, and nuclear accumulation of Stat transcription factors. *J. Biol. Chem.* **279**, 18998–19007 (2004).
10. Mao, X. *et al.* Structural bases of unphosphorylated STAT1 association and receptor binding. *Mol. Cell* **17**, 761–771 (2005).
11. Wenta, N., Strauss, H., Meyer, S. & Vinkemeier, U. Tyrosine phosphorylation regulates the partitioning of STAT1 between different dimer conformations. *Proc. Natl. Acad. Sci. USA* **105**, 9238–9243 (2008).
12. Ptashne, M. *A Genetic Switch: Phage Lambda Revisited* (Cold Spring Harbor Laboratory Press, Plainview, New York, USA, 2004).
13. Lebrecht, D. *et al.* Bicoid cooperative DNA binding is critical for embryonic patterning in *Drosophila*. *Proc. Natl. Acad. Sci. USA* **102**, 13176–13181 (2005).
14. Spitz, F. & Furlong, E.E. Transcription factors: from enhancer binding to developmental control. *Nat. Rev. Genet.* **13**, 613–626 (2012).
15. Lin, J.-X. *et al.* Critical Role of STAT5 transcription factor tetramerization for cytokine responses and normal immune function. *Immunity* **36**, 586–599 (2012).
16. Giorgetti, L. *et al.* Noncooperative interactions between transcription factors and clustered DNA binding sites enable graded transcriptional responses to environmental inputs. *Mol. Cell* **37**, 418–428 (2010).
17. Durbin, J.E., Hackenmiller, R., Simon, M.C. & Levy, D.E. Targeted disruption of the mouse Stat1 gene results in compromised innate immunity to viral disease. *Cell* **84**, 443–450 (1996).
18. Zhong, M. *et al.* Implications of an antiparallel dimeric structure of nonphosphorylated STAT1 for the activation-inactivation cycle. *Proc. Natl. Acad. Sci. USA* **102**, 3966–3971 (2005).
19. Qing, Y. & Stark, G.R. Alternative activation of STAT1 and STAT3 in response to interferon-gamma. *J. Biol. Chem.* **279**, 41679–41685 (2004).
20. Boisson-Dupuis, S. *et al.* Inborn errors of human STAT1: allelic heterogeneity governs the diversity of immunological and infectious phenotypes. *Curr. Opin. Immunol.* **24**, 364–378 (2012).
21. Müller, U. *et al.* Functional role of type I and type II interferons in antiviral defense. *Science* **264**, 1918–1921 (1994).
22. Buchmeier, N.A. & Schreiber, R.D. Requirement of endogenous interferon-gamma production for resolution of Listeria monocytogenes infection. *Proc. Natl. Acad. Sci. USA* **82**, 7404–7408 (1985).

23. Lorsbach, R.B., Murphy, W.J., Lowenstein, C.J., Snyder, S.H. & Russell, S.W. Expression of the nitric oxide synthase gene in mouse macrophages activated for tumor cell killing. Molecular basis for the synergy between interferon-gamma and lipopolysaccharide. *J. Biol. Chem.* **268**, 1908–1913 (1993).

24. Stockinger, S. *et al.* Production of type I IFN sensitizes macrophages to cell death induced by Listeria monocytogenes. *J. Immunol.* **169**, 6522–6529 (2002).

25. Karaghiosoff, M. *et al.* Central role for type I interferons and Tyk2 in lipopolysaccharide-induced endotoxin shock. *Nat. Immunol.* **4**, 471–477 (2003).

26. Hartman, S.E. *et al.* Global changes in STAT target selection and transcription regulation upon interferon treatments. *Genes Dev.* **19**, 2953–2968 (2005).

27. Ramana, C.V., Gil, M.P., Schreiber, R.D. & Stark, G.R. Stat1-dependent and -independent pathways in IFN-gamma-dependent signaling. *Trends Immunol.* **23**, 96–101 (2002).

28. Schmid, C.D. & Bucher, P. MER41 repeat sequences contain inducible STAT1 binding sites. *PLoS ONE* **5**, e11425 (2010).

29. Hu, X. *et al.* Sensitization of IFN-gamma Jak-STAT signaling during macrophage activation. *Nat. Immunol.* **3**, 859–866 (2002).

30. Vinkemeier, U. Getting the message across, STAT! Design principles of a molecular signaling circuit. *J. Cell Biol.* **167**, 197–201 (2004).

31. Lödige, I. *et al.* Nuclear export determines the cytokine sensitivity of STAT transcription factors. *J. Biol. Chem.* **280**, 43087–43099 (2005).

32. Meyer, T., Marg, A., Lemke, P., Wiesner, B. & Vinkemeier, U. DNA binding controls inactivation and nuclear accumulation of the transcription factor Stat1. *Genes Dev.* **17**, 1992–2005 (2003).

33. Bluyssen, H.A. & Levy, D.E. Stat2 is a transcriptional activator that requires sequence-specific contacts provided by Stat1 and p48 for stable interaction with DNA. *J. Biol. Chem.* **272**, 4600–4605 (1997).

34. Sadzak, I. *et al.* Recruitment of Stat1 to chromatin is required for interferon-induced serine phosphorylation of Stat1 transactivation domain. *Proc. Natl. Acad. Sci. USA* **105**, 8944–8949 (2008).

35. Wormald, S., Hilton, D.J., Smyth, G.K. & Speed, T.P. Proximal genomic localization of STAT1 binding and regulated transcriptional activity. *BMC Genomics* **7**, 254 (2006).

36. Segal, E. & Widom, J. From DNA sequence to transcriptional behaviour: a quantitative approach. *Nat. Rev. Genet.* **10**, 443–456 (2009).

37. Kessler, D.S., Veals, S.A., Fu, X.Y. & Levy, D.E. Interferon-alpha regulates nuclear translocation and DNA-binding affinity of ISGF3, a multimeric transcriptional activator. *Genes Dev.* **4**, 1753–1765 (1990).

38. Qureshi, S.A., Salditt-Georgieff, M. & Darnell, J.E. Jr. Tyrosine-phosphorylated Stat1 and Stat2 plus a 48-kDa protein all contact DNA in forming interferon-stimulated-gene factor 3. *Proc. Natl. Acad. Sci. USA* **92**, 3829–3833 (1995).

39. Speil, J. *et al.* Activated STAT1 transcription factors conduct distinct saltatory movements in the cell nucleus. *Biophys. J.* **101**, 2592–2600 (2011).

40. Cheon, H. *et al.* IFNβ-dependent increases in STAT1, STAT2, and IRF9 mediate resistance to viruses and DNA damage. *EMBO J.* **32**, 2751–2763 (2013).

41. Dölken, L. *et al.* High-resolution gene expression profiling for simultaneous kinetic parameter analysis of RNA synthesis and decay. *RNA* **14**, 1959–1972 (2008).

42. Mandal, M. *et al.* Epigenetic repression of the *Igk* locus by STAT5-mediated recruitment of the histone methyltransferase Ezh2. *Nat. Immunol.* **12**, 1212–1220 (2011).

ONLINE METHODS

STAT1F77A mice. To generate mice with the STAT1 polymerization-disrupting substitution STAT1F77A (ref. 43), genomic DNA fragments from an XhoI-digested Sv129/ola mouse genomic P1 artificial chromosome library expressed in *Escherichia coli* DH10B (obtained from the Resource Center of the German Human Genome Project, MPI for Molecular Genetics, Berlin, Germany) were subcloned into the XhoI site of pBluescript (Stratagene). Positive clones encompassing exons 3-5 of the *Stat1* gene were detected by Southern blot analysis using a radioactively labeled probe from HindIII-digested human *STAT1* in pEGFPNI-plasmid[32]. A PCR-amplified 2.9 kb fragment containing exons 3 and 4 was subcloned into NotI–XhoI-digested pd2EGFP1 (Clontech) as the 5′ homology arm. Site-directed mutagenesis (QuikChange site-directed mutagenesis kit, Stratagene) using the primer 5′-CTCTGGAGAATAAT<u>GCC</u>TTGT TGCAGCACAAC-3′ (mutated codon F77 underlined) and the reverse complementary primer was performed as per the manufacturer's recommendations. The mutated fragment was introduced into the NotI–XhoI restriction sites of the pPNTloxPneo vector. The adjacent 3.4 kb genomic fragment containing exon 5 was used as 3′ homology and ligated into the BamHI–KpnI sites of the targeting vector. The resulting construct contained a herpes simplex virus thymidine kinase cassette for negative selection and a neomycin-resistance cassette flanked by two *loxP* sites for positive selection. For transfection, the targeting vector was linearized and electroporated into E14.1 embryonic stem (ES) cells of the 129 mouse strain (Sv129/ola subclone 14.1), which were cultured on feeder layers of mouse embryonic fibroblasts. Cells were grown under double selection (200 µg/ml G418, 2 mM ganciclovir). BamHI-digested genomic DNA from resistant colonies was tested for homologous recombination by Southern hybridization using a 430 bp probe spanning exon 2, which was generated by PCR from mouse genomic DNA with the primer pair 5′-TGCCTCCAGCCCCTTTCCACCA CT-3′ and 5′-GGCAAACCCCATGATGAACCTACA-3′. One clone with a correctly targeted allele at the *Stat1* locus was injected into blastocysts from C57BL/6J mice according to standard techniques. Male chimeric offspring were mated with female Cre deleter mice expressing Cre recombinase to delete the neomycin-resistance cassette. The progeny were screened for absence of the neomycin-resistance cassette by Southern blot using BamHI-digested genomic DNA. Finally, heterozygous *Stat1*[F77A/WT] mice were interbred to generate homozygous *Stat1* F77A animals. The generation of a STAT1F77A mouse strain with a substitution of alanine for phenylalanine in position 77 was confirmed by restriction fragment length polymorphism (RFLP) analyses and DNA sequencing of genomic DNA. RFLP was detected using Tsp509I digestion of a 282 bp PCR product (primer pair: 5′-CGCGAATTGCTAATAAAACA-3′ and 5′-TGCTGCTGAGTCCAAATAAAG-3′). Restriction with Tsp509I generated a ~50 bp fragment with both wild-type- and STAT1F77A-derived PCR products. Due to the loss of a Tsp509I site caused by mutation F77A, the STAT1F77A-derived DNA showed an additional 234 bp fragment, which was cleaved into 110 bp and 120 bp fragments with wild-type-derived DNA. For DNA sequencing nested PCR with primers 5′-TGCGACCATCCGCTTCCATGACC-3′ and 5′-TTTCAATGCCCAGTGAGCGTGCA-3′ was done, whereby the latter was also used for sequencing. The mice were crossed on C57BL/6J background for ten generations.

Animal experimentation. All *in vivo* experiments with mice were approved by the local animal experimentation ethics committee (V54-19c20/15c MR 20/11, Regierungspräsidium Gießen, Germany) and carried out in accordance with the German Animal Protection Act. For bacterial challenge, *L. monocytogenes* LO28 strain was grown in BHI broth (Difco) to late logarithmic phase as measured by an OD of 0.8 at 600 nm[44]. Bacteria were pelleted and washed four times with PBS, before mice were intraperitoneally injected with *L. monocytogenes* at 1×10^6 cells per animal. The infectious dose was controlled by plating serial dilutions on BHI agar plates. For intranasal virus infection, mice were anesthetized with isoflurane and a total of 10 µl containing 10^4 p.f.u. of VSV-Indiana (Mudd-summers strain) in PBS were pipetted into both nostrils[45]. For the *in vivo* LPS challenge, mice were injected intraperitoneally with 10 mg/kg of body weight of *E. coli* LPS (0111:B4) purified by phenol extraction (Sigma-Aldrich, L2630). The cohorts consisted of male littermates aged 8-12 weeks obtained from crossings of STAT1F77A heterozygous mice. Sample sizes were chosen using power calculations, with power level settings of 0.8 and an anticipated effect size (Cohen's *d*) of 0.95, resulting in a minimum

group size of $n = 15$. No exclusion criteria were defined and no animals used in the experiments reported were excluded from the data analyses. Survival data were recorded by staff blinded to the genotype of the different cohorts. The experiments were not randomized.

Cell culture and cytokines. Wild-type and STAT1F77A embryonic fibroblasts from crossings of STAT1F77A heterozygous mice were prepared from 13.5-day-old embryos by standard methods and were genotyped by RFLP analysis and genomic DNA sequencing as described. Cells were immortalized with Simian Virus 40 (SV40) large T antigen. Generation of bone marrow macrophages and nitric oxide determination (Griess assay, Promega) were as described[46]. Growth of *L. monocytogenes* in macrophages was determined by colony-forming unit (c.f.u.) assay as described[47]. In brief, cells were infected at MOI 10 and lysed with distilled water at the indicated time points. Bacterial c.f.u. were determined by plating serial dilutions of the lysates on brain heart infusion (BHI) agar. The death of macrophages infected with *L. monocytogenes* at MOI 10 was determined after a 24 h culture period. Propidium iodide uptake by dead cells was quantified by flow cytometry[47]. MEFs and HeLa-S3 cells (obtained from Deutsche Sammlung von Mikroorganismen und Zellkulturen GmbH, Braunschweig, Germany) were kept in growth medium, DMEM supplemented with 10% FBS and 1% penicillin/streptomycin, in a humidified incubator with 5% CO_2 at 37 °C. Cells were free of mycoplasma contamination as tested by DAPI indirect DNA stain (Sigma D9542). Mouse IFN-α and IFN-γ were obtained from Calbiochem, human IFN-γ from Merck Biosciences, and human IFN-α from PBL Biomedical Laboratories.

Cell extractions, SDS-PAGE and immunoblotting. MEF and HeLa whole cell extracts were generated as described[48]. Spleen homogenates were prepared from spleens removed from both wild-type and STAT1F77A mice immediately after culling. Spleens were homogenized in lysis buffer (30 mM Tris-HCl, pH 8.8, 8 M urea, 4% CHAPS, 1× Roche Complete protease inhibitor) using 1.4 mm ceramic beads (Lysing Matrix D, MP Biomedicals) in a Fast Prep 24 homogenizer (MP Biomedicals). The soluble homogenate was retrieved after centrifugation. SDS-PAGE and quantitative immunoblotting using a Li-Cor Odyssey infra red detection system was as described[49]. Immunoblotting results were obtained by consecutive probing with the indicated antibodies, whereby immunoglobulins were removed after probing by incubation for 60 min at 65 °C in stripping buffer (25 mM glycine, 2% SDS, pH 2.0). The following antibodies were used at the indicated dilutions: anti-mouse STAT1α (Santa Cruz, sc-591; 1:4,000), anti-human STAT1 (Santa Cruz sc-345; 1:4,000), anti-Tyr701-phosphorylated STAT1 (Cell Signaling, #9171; 1:1,000), anti-Ser727-phosphorylated STAT1 (Invitrogen, #44-382G; 1:1,000), anti-STAT2 (Santa Cruz, sc-950; 1:1,000), anti-Tyr688-phosphorylated STAT2 (Millipore, 07-224; 1:1,000), anti-IRF9 (Cambridge Biosciences, AP11875a; 1:1,000), anti-GFP (Santa Cruz, sc-8334; 1:1,000), anti-β-actin (Sigma, A5441; 1:8,000), IRdye800CW-conjugated anti-mouse (#926-32212; 1:10,000) and anti-rabbit (#926-32213; 1:10,000) IgG secondary antibodies were purchased from Li-Cor Bioscience.

Microarrays. Wild-type or STAT1F77A primary MEFs were kept for 15 h in serum-reduced DMEM (1% FBS) to discern expression profiles in the absence of mitogenic stimuli. Subsequent stimulation with IFN-α (1,000 U/ml) or IFN-γ (50 U/ml) was for 6 h. Total RNA from untreated and IFN-treated MEFs (1.1×10^6 cells per sample) was isolated using the Absolutely RNA Miniprep kit according to the manufacturer's recommendations (Agilent). RNA was labeled with Cy3 or Cy5 dyes using Two-color RNA Spike-In kit (Agilent), and hybridized to whole mouse genome microarrays (4×44k, Agilent) using Agilent's Gene Expression Hybridization kit, Microarray Hybridization Chamber kit, and the microarray hybridization oven (Agilent) as per the manufacturer's protocol. The hybridized arrays were scanned with Agilent G2565CA microarray scanner. Raw microarray image files were read and normalized with Agilent's Feature Extraction software Version 10.7.1.1 and protocol template GE2_107_Sep09 using defaults for all parameters. Data were analyzed with GenespringGX software (Agilent); probes with intensity changes greater than 2-fold on the $\log_2$ scale were considered as IFN-regulated genes. Mean log ratios were used for genes recognized by multiple probes.

Quantitative reverse transcriptase polymerase chain reaction (qRT-PCR). Immortalized MEFs were kept in serum reduced (1%) growth medium for 15 h before change to growth medium containing IFN-α (1,000 U/ml) or IFN-γ (50 U/ml). Unless stated otherwise, treatment with IFN was for 6 h. Priming of cells with IFN-γ was achieved by keeping them for 24 h in growth medium with 1 U/ml IFN-γ. After another 2 h in growth medium, cells were treated with 50 U/ml IFN-γ for 6 h. The unprimed control cells shown in **Figure 5** were kept in growth medium throughout. RNA extraction and qRT-PCR was done using QantiTect SYBR Green PCR kit as described[46]. The primers pairs used are listed in **Supplementary Table 5**.

Electrophoretic mobility shift assay (EMSA). MEFs were left untreated or treated for 60 min with IFN-α (1,000 U/ml) or IFN-γ (50 U/ml). Cytoplasmic and nuclear cell extractions and protein determination were as described[49]. For EMSA, cytoplasmic and nuclear extracts were combined and quantitative immunoblotting was done to determine the content of Tyr701-phosphorylated STAT1 in wild-type- and STAT1F77A-derived cell extracts. They were then normalized for Tyr701-phosphorylated STAT1 by dilution with untreated extracts from cells of the same genotype. Probes were labeled with 80 μCi/ml α-[32P]-dNTPs (10 mCi/mL, 6,000 Ci/mmol) (PerkinElmer) and 5 U exonuclease-negative Klenow DNA polymerase (NEB). The DNA binding reaction and native polyacrylamide gel electrophoresis were as described[49]. The following probes with 5′-TGAC-3′ overhangs at the 5′ ends were used. GAS (M67)[4], 5′-CGACATTTCCCGTAAATCTG-3′ and 5′-CAGA TTTACGGGAAATGTCG-3′; 2×GAS, 5′-CGTTTCCCCGAAATTGACGGA TTTCCCCGAAACG-3′ and 5′-CGTTTCGGGGAAATCCGTCAATTTCGG GGAAACG-3′; ISRE (ISG15)[38], 5′-GGGAAAGGGAAACCGAAACTGA-3′ and 5′-TTCAGTTTCGGTTTCCCTTTCCC-3′; 2×ISRE, 5′-GGGAAAGG GAAACCGAAACTGAAATTGGGGAAAGGGAAACCGAAACTGAA-3′ and 5′-TTCAGTTTCGGTTTCCCTTTCCCCAATTTCAGTTTCGGTTTC CCTTTCCC-3′. The protein composition of IFN-induced nucleoprotein complexes was determined by supershift assay using STAT1 (Santa Cruz, sc-591; diluted 1:1,000), STAT2 (Santa Cruz, sc-950; diluted 1:1,000), or STAT3 (Santa Cruz, sc-482; diluted 1:1,000) antibodies as described[49] (results not shown). Competition EMSA was done as described using 500-fold molar excess of unlabeled probe[4].

Chromatin immunoprecipitation. Chromatin immunoprecipitation assays (ChIP) were performed using the Magna ChiP kit (Millipore, MAGNA0001) as per the manufacturer's instructions with the following modifications. Three confluent 15-cm dishes of immortalized WT or KI MEFs (1×10^7 cells) were treated for 45 min with IFN-α (1,000 U/ml) or IFN-γ (50 U/ml). Cells were crosslinked with 1% formaldehyde for 10 min at 21 °C, followed by the addition of 0.4 M glycine and incubation for another 5 min. The chromatin was sheared mechanically using Bioruptur sonicator (10 cycles, each with 30 s pulse and 30 s pause, power setting 'high'). Immunoprecipitations with chromatin from 1×10^6 cells in a volume of 0.5 ml buffer and 5 μg of antibody were done for 16 h at 4 °C using anti-STAT1 (Santa Cruz, sc-591X), anti-STAT2 (Santa Cruz, sc-839X), anti-IRF9 (Bethyl, #A303-387A), anti-acetylated histone 3 (Millipore, 06-599B) and anti-unspecific IgG (Millipore, PP64B). The primers pairs used in the PCR following ChIP are listed in **Supplementary Table 6**.

Quantitative cell imaging. Plasmids pSTAT1-F77A-GFP[9], pSTAT1-DNA^minus^-GFP[32], pSTAT1DNA^plus^-GFP[32] and pSTAT1-NES-GFP[31] are described. C-terminal fusion of STAT1 with NES and GFP moieties does not affect DNA binding to GAS sites[50]. Plasmids pSTAT1-DNA^minus^-NES-GFP and pSTAT1-DNA^plus^-NES-GFP were generated by transferring the HindIII insert from pSTAT1-DNA^minus^-GFP or pSTAT1DNA^plus^-GFP into pSTAT1-NES-GFP cut by the same enzyme. Plasmids pSTAT1-F77A-DNA^minus^-NES-GFP and pSTAT1-F77A-DNA^plus^-NES-GFP were generated by transferring the BglII–SpeI insert from pSTAT1-F77A-GFP into pSTAT1-DNA^minus^-NES-GFP

and pSTAT1-DNA^plus^-NES-GFP, both cut with the same enzymes. STAT1-NES-GFP and the derivatives thereof used in this study showed similar tyrosine phosphorylation in response to IFN stimulation (not shown). For cell imaging, ~80% confluent HeLa cells were transfected using Lipofectamine. After 24 h the cells were stimulated for 60 min with IFN-γ (50 U/ml) or IFN-α (1,000 U/ml) followed by fixation for 15 min in −20 °C MeOH in phosphate-buffered saline. Cells were examined with a Leica TCP-SP2 confocal microscope using an argon laser (Ar/ArKr) for GFP excitation at 488 nm. Fluorescence emission at 476 nm was recorded in a 1 μm thick optical slice through the cell nucleus median using circular regions of interest (ROI, 0.5 μm radius), whereby nucleoli were omitted. Five ROIs per cell were recorded and their means were used in **Figure 6a**. Included in the analyses were only cells with similar cytoplasmic GFP signal intensities within the dynamic detection range, namely in between 150 and 200 light units. Sample size was chosen using power calculations, with power level settings of 0.8 and an anticipated effect size (Cohen's *d*) of 0.5, resulting in a minimum group size of $n = 51$.

Statistical analyses. Continuous data are presented as means and standard deviation or fold change. Survival data are shown as Kaplan Meier curves with log-rank tests (Mantel-Cox) for the comparison between samples. *P*-values of less than 0.05 were used to indicate statistical significance. Data were analyzed on a personal computer with SPSS 19.0 for Windows (SPSS Inc.).

Promoter sequence analyses. Putative regulatory genomic regions were defined by non-overlapping sequences 3 kb upstream and 500 bp downstream relative to the start position(s) of the corresponding gene in RefSeq transcript annotations on the mm9 mouse genome assembly, as downloaded using the UCSC table browser on 29 January 2013 (ref. 51). GAS sites were identified by scoring of a STAT1 PWM derived from ChIP-seq data[28]. The maximal PWM score of an optimal STAT1 binding site is 42 (ref. 28); ChIP-seq data indicate binding site occupancy exceeding background values with PWM scores above 25 (ref. 28). **Supplementary Figure 6** provides representative sequences for PWM scores 21, 25, 32, and 40. Multiple GAS were identified by applying the criteria of each GAS having a PWM score >20 with a center-to-center distance <31 bp. Experimental *in vitro* data indicate that STAT1 cooperative DNA binding can occur over distances of 18 or 23 bp[4]. This agrees with ChIP-seq data for non-repetitive genomic DNA demonstrating that tandemly arranged GAS sites are most frequently separated by 18-21 bp[28]. ISGF3 binding sites were predicted by SABiosciences' text mining application at http://www.sabiosciences.com/chipqpcrsearch.php?app=TFBS.

43. Chen, X. *et al.* A reinterpretation of the dimerization interface of the N-terminal domains of STATs. *Protein Sci.* **12**, 361–365 (2003).
44. Stockinger, S. *et al.* Characterization of the interferon-producing cell in mice infected with Listeria monocytogenes. *PLoS Pathog.* **5**, e1000355 (2009).
45. Detje, C.N. *et al.* Local type I IFN receptor signaling protects against virus spread within the central nervous system. *J. Immunol.* **182**, 2297–2304 (2009).
46. Begitt, A., Droescher, M., Knobeloch, K.P. & Vinkemeier, U. SUMO conjugation of STAT1 protects cells from hyperresponsiveness to IFNγ. *Blood* **118**, 1002–1007 (2011).
47. Zwaferink, H., Stockinger, S., Reipert, S. & Decker, T. Stimulation of inducible nitric oxide synthase expression by beta interferon increases necrotic death of macrophages upon *Listeria monocytogenes* infection. *Infect. Immun.* **76**, 1649–1656 (2008).
48. Pelzel, C., Begitt, A., Wenta, N. & Vinkemeier, U. Evidence against a role for β-arrestin1 in STAT1 dephosphorylation and the inhibition of interferon-γ signaling. *Mol. Cell* **50**, 149–156 (2013).
49. Antunes, F., Marg, A. & Vinkemeier, U. STAT1 signaling is not regulated by a phosphorylation-acetylation switch. *Mol. Cell. Biol.* **31**, 3029–3037 (2011).
50. Meyer, T., Begitt, A. & Vinkemeier, U. Green fluorescent protein-tagging reduces the nucleocytoplasmic shuttling specifically of unphosphorylated STAT1. *FEBS J.* **274**, 815–826 (2007).
51. Meyer, L.R. *et al.* The UCSC Genome Browser database: extensions and updates 2013. *Nucleic Acids Res.* **41**, D64–D69 (2013).

Corrigendum: STAT1-cooperative DNA binding distinguishes type 1 from type 2 interferon signaling

Andreas Begitt, Mathias Droescher, Thomas Meyer, Christoph D Schmid, Michelle Baker, Filipa Antunes, Markus R Owen, Ronald Naumann, Thomas Decker & Uwe Vinkemeier

In the version of this article initially published, Klaus-Peter Knobeloch was incorrectly not included in the author list or Author Contributions section. This name should appear after "Filipa Antunes" in the author list and should be linked to the following affiliation: Institut für Neuropathologie, Universitätsklinikum Freiburg, Freiburg, Germany. The Author Contributions section should include the following revision to the sixth item: "K.-P.K. and R.N. contributed reagents and expertise for mouse genetics experiments" (and the thanks to " K.-P. Knobeloch, Universität Freiburg, for advice and cloning reagents" should be removed from the Acknowledgments section). The error has been corrected in the HTML and PDF versions of the article.